



## OPEN ACCESS

## EDITED BY

Z. Carl Lin,  
Harvard Medical School, United States

## REVIEWED BY

Jinlong Huo,  
Yunnan Agricultural University, China  
Jianlei Gu,  
Yale University, United States

## \*CORRESPONDENCE

M. F. Miles,  
✉ michael.miles@vcuhealth.org

RECEIVED 27 June 2024

ACCEPTED 29 August 2024

PUBLISHED 11 September 2024

## CITATION

Gnatowski ER, Jurmain JL, Dozmorov MG, Wolstenholme JT and Miles MF (2024) Ninein, a candidate gene for ethanol anxiolysis, shows complex exon-specific expression and alternative splicing differences between C57BL/6J and DBA/2J mice.  
*Front. Genet.* 15:1455616.  
doi: 10.3389/fgene.2024.1455616

## COPYRIGHT

© 2024 Gnatowski, Jurmain, Dozmorov, Wolstenholme and Miles. This is an open-access article distributed under the terms of the [Creative Commons Attribution License \(CC BY\)](https://creativecommons.org/licenses/by/4.0/). The use, distribution or reproduction in other forums is permitted, provided the original author(s) and the copyright owner(s) are credited and that the original publication in this journal is cited, in accordance with accepted academic practice. No use, distribution or reproduction is permitted which does not comply with these terms.

# Ninein, a candidate gene for ethanol anxiolysis, shows complex exon-specific expression and alternative splicing differences between C57BL/6J and DBA/2J mice

E. R. Gnatowski<sup>1,2</sup>, J. L. Jurmain<sup>1</sup>, M. G. Dozmorov<sup>2,3</sup>,  
J. T. Wolstenholme<sup>1,2</sup> and M. F. Miles<sup>1,2\*</sup>

<sup>1</sup>Department of Pharmacology and Toxicology, Virginia Commonwealth University, Richmond, United States, <sup>2</sup>VCU Alcohol Research Center, Virginia Commonwealth University, Richmond, United States, <sup>3</sup>Department of Biostatistics, Virginia Commonwealth University, Richmond, United States

Ethanol's anxiolytic actions contribute to increased consumption and the development of Alcohol Use Disorder (AUD). Our laboratory previously identified genetic loci contributing to the anxiolytic-like properties of ethanol in BXD recombinant inbred mice, derived from C57BL/6J (B6) and DBA/2J (D2) progenitor strains. That work identified *Ninein* (*Nin*) as a candidate gene underlying ethanol's acute anxiolytic-like properties in BXD mice. *Nin* has a complex exonic content with known alternative splicing events that alter cellular distribution of the NIN protein. We hypothesize that strain-specific differences in *Nin* alternative splicing contribute to changes in *Nin* gene expression and B6/D2 strain differences in ethanol anxiolysis. Using quantitative reverse-transcriptase PCR to target specific *Nin* splice variants, we identified isoform-specific exon expression differences between B6 and D2 mice in prefrontal cortex, nucleus accumbens and amygdala. We extended this analysis using deep RNA sequencing in B6 and D2 nucleus accumbens samples and found that total *Nin* expression was significantly higher in D2 mice. Furthermore, exon utilization and alternative splicing analyses identified eight differentially utilized exons and significant exon-skipping events between the strains, including three novel splicing events in the 3' end of the *Nin* gene that were specific to the D2 strain. Additionally, we document multiple single nucleotide polymorphisms in D2 *Nin* exons that are predicted to have deleterious effects on protein function. Our studies provide the first in-depth analysis of *Nin* alternative splicing in brain and identify a potential genetic mechanism altering *Nin* expression and function between B6 and D2 mice, thus possibly contributing to differences in the anxiolytic-like properties of ethanol between these strains. This work adds novel information to our understanding of genetic differences modulating ethanol actions on anxiety that may contribute to the risk for alcohol use disorder.

## KEYWORDS

Ninein, alternative splicing, RNAseq, exon skipping, ethanol, anxiety, mouse genetics

## Introduction

The acute behavioral responses to ethanol in both humans and animal models include anxiolysis. Both clinical and preclinical research has demonstrated that the anxiolytic effects of acute ethanol consumption can lead to increased alcohol intake and play a critical role in the development of alcohol use disorder (AUD) (Schuckit and Smith, 1997; Becker, 2017). Ethanol's anxiolytic properties are believed to enhance its reinforcing effects, resulting in a more pronounced response to ethanol in individuals who exhibit greater susceptibility to stress or anxiety compared to those with lower levels of anxiety (Becker, 2017; Schuckit and Hesselbrock, 1994). This enhanced anxiolytic response could result in a greater predisposition to consume alcohol, ultimately aiding development of alcohol use disorder (AUD). Furthermore, ethanol's anxiolytic properties generate a potential feed-forward action on ethanol consumption due to the increase in anxiety seen upon withdrawal in AUD subjects (Heilig et al., 2010; Schuckit and Hesselbrock, 1994). The genetic variance underlying ethanol's anxiolytic effects could thus influence both the development of AUD as well as relapse during ethanol withdrawal.

Using a 2-stage quantitative trait loci (QTL) mapping in BXD recombinant inbred (RI) mice, *Ninein* (*Nin*) was previously identified as a candidate gene for a Chr 12 QTL (*Etanq1*) associated with ethanol's anxiolytic-like properties in the light-dark box transitional model of anxiety (Putman et al., 2016). BXD RI strains are derived from C57BL/6J (B6) and DBA/2J (D2) inbred progenitor mouse strains which exhibit contrasting responses across multiple ethanol-related behaviors (Belknap et al., 1993). Supportive studies on *Nin* as a candidate gene revealed a *Nin* cis-expression QTL at the location of the *Etanq1* behavioral QTL, and higher mRNA expression in D2 progenitors compared to B6 in nucleus accumbens (NAc), suggesting that genetic differences in D2 mice caused higher *Nin* expression, which the anxiolytic-like actions of ethanol in the light-dark box (Putman et al., 2016). Protein expression analysis identified significantly higher expression of two provisional *Ninein* isoforms in D2 mice compared to B6 animals, thus implicating potential differences in splicing between these two strains (Putman et al., 2016). However, the full documentation and characterization of these potential splicing differences in *Nin* expression between B6 and D2 mice remain to be determined.

*Ninein* is a microtubule-associated protein that plays a role in microtubule organization at the centrosome and in the cytoplasm (Mogensen et al., 2000; Baird et al., 2004). *Ninein* associates with the centrosome in many cell types, where it recaptures minus-ends of microtubules and is essential for apico-basal microtubule formation characteristic of complex polarized cells such as neurons (Goldspink et al., 2017; Baird et al., 2004). *Ninein* has primarily been studied in the context of development and has been demonstrated to undergo extensive alternative splicing that influences neural progenitor cells (NPCs) differentiation into neurons (Zhang et al., 2016). Previous published reports have identified roles of specific *Nin* exons that contribute localization and function during development (Zhang et al., 2016). In human disease, *Nin* has been associated with Seckel Syndrome (<https://hpo.jax.org/browse/disease/OMIM:614851>), which has multiorgan developmental abnormalities including

cognitive impairment, and also with schizophrenia (Bigdeli et al., 2021). *Ninein* expression has also been found to be regulated by a history of cocaine use in human postmortem hippocampus and dorsal lateral prefrontal cortex (Farris et al., 2015; Ribeiro et al., 2017). Understanding the role of *Nin* alternative splicing in adult animals may contribute to characterizing its role in regulating ethanol's anxiolytic properties.

RNA splicing is a post-transcriptional modification that plays a critical role in mammalian gene expression (Ule and Blencowe, 2019). This process involves the removal of introns from newly transcribed pre-mRNA sequences and is essential for generating mature protein-coding mRNAs. Compared to constitutive splicing, alternative splicing events comprise multiple processes that result in the inclusion or exclusion of specific exons in numerous combinations leading to the generation of multiple unique mRNA and protein isoforms from a single gene (Wang et al., 2015). These processes generate transcriptome-wide complexity that can occur under both physiological and pathophysiological conditions. The human brain demonstrates a significantly higher occurrence of alternative splicing events that are evolutionarily conserved, demonstrating a functional role of alternative isoforms in the brain (Nikom and Zheng, 2023; Yeo et al., 2004). There are five basic modes of alternative splicing: exon skipping (or cassette-type alternative exon), mutually exclusive exons, alternative 3' splice site, alternative 5' splice site, and intron retention. Exon skipping is the most prevalent pattern of alternative splicing in vertebrates and invertebrates (Lee and Rio, 2015).

Our prior work strongly implicates *Nin* as a candidate gene underlying a Chr 12 QTL for ethanol anxiolytic-like behavioral responses in BXD mice, and that this may involve both genetic regulation of *Nin* expression and splicing. In order to characterize potential mechanisms of *Nin* expression differences more fully between the BXD progenitor strains, B6 and D2 mice, we studied strain-specific differences in exon utilization and splicing using selective quantitative RT-PCR and RNAseq analysis. By conducting deep sequencing of RNA transcripts, we identified novel strain-specific *Nin* alternative splicing and exon-utilization events in B6 and D2 adult mice. Our data demonstrate strain differences in previously reported exon 18 expression and splicing, as well as inclusion of novel protein coding exons in the D2 strain within the 3' region of the genome. Furthermore, we confirm potentially important coding region polymorphisms in D2 mice that might also alter *Nin* splicing and function. This evaluation of alternative splicing of a QTL derived candidate gene provides an initial framework for investigating the functional basis of strain-specific gene expression and demonstrates the potential complexity of genetic differences modulating complex behaviors such as AUD.

## Methods

### Animal subjects

Male C57BL/6J and DBA/2J mice were obtained from the Jackson Laboratory (Bar Harbor, ME, United States) at 7–8 weeks of age and habituated to the vivarium for at least 1 week prior to initiating experimental studies. Animals were

group-housed (four animals per cage with *ad libitum* access to food and water, under a 12-h light/dark cycle, in a 21°C environment). All experiments were approved by the Institutional Animal Care and Use Committee of Virginia Commonwealth University and followed the National Institutes of Health Guidelines for the Care and Use of Laboratory Animals. At 9 weeks of age, animals were sacrificed by cervical dislocation and decapitation. Immediately thereafter, brains were extracted and chilled for 1 min in cold phosphate buffered saline before brain regions being punch or wedge micro-dissected from 2 µm thick coronal slices as previously described (Kerns et al., 2005) for medial prefrontal cortex (mPFC), nucleus accumbens (NAc), and Amygdala (Amy) sections. Excised regions were placed in individual tubes, flash-frozen in liquid nitrogen, and stored at -80°C prior to use for RNA extraction and analysis as below.

## RNA extractions

Samples were homogenized with a Polytron® (Kinematica AG, Malters, Switzerland) and total RNA was extracted using a guanidine/phenol/chloroform method (STAT-60, Tel-Test, Inc. Friendswood, TX, United States) as per manufacturer guidelines. Each RNA liquid layer was added to a miRNeasy Mini Column (Cat #: 217004, Qiagen, Hilden, Germany) for cleanup and elution of total RNA. RNA concentration was determined by measuring absorbance at 260 nm using a Nanodrop 2000 (Thermo Scientific). RNA quality and purity was assessed by 260/280 absorbance ratios and by electrophoresis using the Agilent 2100 Bioanalyzer (Agilent Technologies, Savage, MD, United States). Samples all had RNA Integrity Numbers (RIN) ≥ 8 and 260/280 ratios between 1.96 and 2.05.

## Quantitative reverse transcriptase PCR

500 ng of RNA was converted to cDNA using the iScript cDNA synthesis kit (#1708891, Bio-Rad, Hercules, CA, United States) according to the manufacturer's instructions. All cDNA samples were diluted to ~1 ng/µL prior to PCR. qRT-PCR was performed using the Bio-Rad CFX Connect thermocycler according to manufacturer's instructions for iTaq™ Universal SYBR® Green Supermix (#1725124, Bio-Rad, Hercules, CA, United States). Primers (Eurofin Genomics, Luxembourg) efficiencies were between 90% and 110% and each primer set resulted in only one PCR product on gel electrophoresis. Primer sequences, amplicon sizes, and annealing temperatures (T<sub>m</sub>) used for each gene are listed in [Supplementary Table S1](#). Data analysis was performed using the 2<sup>-[ΔΔCT]</sup> method (Heid, 1996). Relative mRNA expression was normalized to housekeeping genes Ublcp1, Sort1, and Ppp2r2a, and Stab2 was used as a strain control. Ublcp1 was excluded in the amygdala after seeing significant strain differences in expression. Statistical analysis of qRT-PCR data was performed using a student's t-test between strains within each brain region. For agarose gel electrophoresis, PCR products were analyzed using TrackIt 50bp DNA ladder (Invitrogen, Cat. #10488043) for sizing

and gels imaged using the Biorad GelDoc System (Bio-Rad, Cat. #1704486).

## RNAseq library preparation and sequencing

Library preparation and sequencing were completed by the VCU Genomics Core. A total of five biological replicates were obtained from each strain. Preparation of cDNA libraries was conducted using the standard protocols for the Illumina Stranded mRNA Prep, Ligation Kit (#20040534, Illumina, San Diego, CA, United States). Library insert size was determined using an Agilent Bioanalyzer. Libraries were sequenced on the Illumina NextSeq 2000 (Illumina, San Diego, CA, United States) with 150 bp paired-end reads for a target depth of 100 million reads per sample. All RNAseq raw and data and processed read counts have been submitted to the Gene Expression Omnibus (GEO) database (GEO accession #GSE274854) (<https://www.ncbi.nlm.nih.gov/geo/query/acc.cgi?acc=GSE274854/>).

## RNAseq quality control and alignment

Initial quality control checks were performed by FastQC (<https://github.com/s-andrews/FastQC>). All samples showed mean quality scores > 30. Fastp v. 0.22.0 (Chen et al., 2018) was used for adapter and end trimming and further quality control prior to alignment. B6 and D2 samples were aligned to release 108 of the Ensembl genome for C57BL/6J mice using STAR (v 2.7.10b) with the following parameters: “--readFilesCommand zcat,” to uncompress. gz files, “--outSAMtype BAM SortedByCoordinate,” to output as a sorted BAM file, “--outReadsUnmapped Fastx,” to output unmapped reads into separate files, “quantMode GeneCounts,” to count the number of reads per gene while mapping, and “--bamRemoveDuplicatesType UniqueIdenticalNotMulti” to mark duplicate unique mappers but not multimappers (Dobin and Gingeras, 2016). Aligned BAM files produced by STAR were further sorted by coordinate using Samtools v 1.6 (Li et al., 2009). Raw read counts for each BAM file were assigned and quantified using FeatureCounts (Liao et al., 2014). A summary of RNAseq metrics can be found in [Supplementary Table S2](#).

## Differential gene expression analysis

Count files were analyzed for differential gene expression between B6 and D2 animals using the R package DESeq2 v 1.36.0 (Love et al., 2014). Low expressed genes where the median across all samples is zero were eliminated prior to analysis. Principal Component Analysis of the variance on the top 10,000 genes was run to identify significant sample outliers. Genes with a false discovery rate (FDR) < 0.05 were considered significantly altered and used in downstream analyses.

## Differential exon usage analysis

A GFF annotation file containing collapsed exon counting bins was prepared from the UCSC GRCm39/mm39 GTF file using DEXSeq v. 1.42.10 (Anders et al., 2012). Python script *dexseq\_prepare\_annotation.py*. The number of reads overlapping each exon

bin was then counted using the DEXSeq Python script *dexseq\_count.py*, the GFF file, and each sample's BAM file. Differential exon usage (DEU) analysis was then carried out for the same contrasts studied in our DGE analysis using the DEXSeq R package standard analysis workflow. For analysis of Ninein differential exon usage, we utilized an FDR < 0.2 to identify significantly altered exon events.

## BXD amygdala exon-level expression data

To further evaluate the relationship between Ninein exon expression and acute ethanol anxiolytic-like activity, we compared our DEXSeq results with the amygdala exon-level dataset in GeneNetwork (INIA Amygdala Exon Affy MoGene 1.0 S T (Nov10) RMA) (Mulligan et al., 2017). This dataset provides estimates of mRNA expression in the Amygdala of 58 genetically diverse strains including 54 BXD Recombinant inbred strains, two F1 hybrid strains (B6D2F1 and D2B6F1), and the two progenitor strains (C57BL/6J and DBA/2J). 33 coding exons were correlated with the Top 500 BXD Phenotypes and filtered for Pearson correlations with previous ethanol light-dark box ethanol anxiolytic-like activity data from our prior studies in BXD mice (Putman et al., 2016). Exons were correlated with acute ethanol phenotypes from the light dark box (LDB) transitional model of anxiety for percent distance traveled in the light (%DTL) or percent time spent in the light (%TIL) in response to an acute dose of ethanol (1.8 g/kg) at either 5-min or 10-min intervals.

## Alternative splicing analysis

Analysis of *Nin* exon utilization and splicing focused on five fundamental alternative splicing events: exon skipping, alternative 5' and 3' splice sites, mutually exclusive exons, and intron retention. Junction read counts for alternative splicing events were quantified by rMATS v. 4.1.2 (Shen et al., 2014) utilizing the STAR alignment BAM files as input. An FDR cutoff of 0.2 was used to identify significant alternative splicing events. *P*-values and FDRs that are smaller than the numerical accuracy cutoff ( $p < 2.2E-16$ ) register as 0 in the rMATS output (see Supplementary Table S4). Rmats2sashimiplot v 2.0.4 (within rMATS) and Maser v 1.14.0 (Kinjo et al., 2018) were used to analyze and visualize rMATS outputs.

Regtools v. 0.5.2 (Cotto et al., 2023) was used to quantify junction reads and annotate novel/unusual junctions using the "junctions annotate" function. Outputs include chromosome junction start and end coordinates, as well as a score indicating the number of reads supporting the junction. Junctions were filtered again to identify novel splice junctions contain either a novel donor (D), a novel acceptor (A), a novel donor and novel acceptor pair (NDA), or no known donor or acceptor (N). Junctions with both a median score greater than one and a mean score greater than one across all 10 samples were included for statistical analysis. Scores across all 10 samples were compared using a student's *t*-test and Bonferroni correction for multiple testing across the number of junctions passing filtering.

## Single nucleotide polymorphism (SNP) analysis

To analyze single nucleotide polymorphisms (SNPs), we used the Mouse Genome Informatics (MGI) (Blake et al., 2021; Baldarelli et al., 2021) and Ensembl (Martin et al., 2023) databases using the GRCm39 assembly. The MGI database was used to output specific SNPs differing in the *Nin* gene from chr 12: 70,058,297–70,159,961 and the Ensembl Database to identify the variant type and overlapping regulatory regions.

## Results

### D2 mice exhibit increased ninein mRNA expression

We selected C57BL/6J (B6) and DBA/2J (D2) mice for our studies because of their distinct ethanol-related behaviors and status as progenitor strains for the BXD RI strains that were used in identification of *Nin* as a candidate gene for ethanol-anxiolysis. Total RNA was isolated from ethanol-naïve male B6 and D2 mice from the nucleus accumbens (NAc), medial prefrontal cortex (mPFC), and amygdala (AMY) for evaluating *Nin* alternative splicing events using qRT-PCR (Figure 1). Primers were designed to target different *Nin* exons reflective of known *Nin* transcript variants. Primer labels containing a (+) represent the inclusion of that exon in the primer design. Primer labels containing a (–) represent the exclusion of that exon from primer design and subsequent transcripts. These primer targets are defined according to the canonical *Nin* transcript (Figure 2; Ensemble ID: ENSMUST00000085314.11) and included the canonical 3' untranslated region, the alternative 5' splice site at exon 28 (Ensemble IDs: ENSMUST00000085314.11 and ENSMUST0000022237.2), transcripts excluding exon 18 (Ensemble IDs: ENSMUST00000220689.2 and ENSMUST00000222835.2), and transcripts including exon 29 (Ensemble IDs: ENSMUST00000220689.2 and ENSMUST00000223257.2) (Figure 1; Supplementary Table S1). Primers investigating exon 28 targeted the shortened splice form of the exon.

In mPFC (Figure 1A), D2 mice ( $n = 10$ ) exhibited a significantly higher expression of exon 18 (–) ( $p = 0.021$ ), exon 28 A<sup>5</sup>SS ( $p = 2.85E-05$ ) and exon 29 (+) ( $p = 0.0047$ ). B6 mice ( $n = 10$ ) showed significantly higher expression of the 3' UTR region ( $p = 0.0038$ ) of *Nin*. This same pattern of expression was seen in the NAc (Figure 1B) where D2 mice ( $n = 5$ /strain) showed significantly higher expression of exons 28 A<sup>5</sup>SS ( $p = 0.01$ ), exon 29 (+) ( $p = 0.009$ ), and exon 18 (–) ( $p = 0.02$ ), and B6 mice showed significantly higher expression of the 3' UTR region ( $p = 0.00011$ ). In the amygdala (Figure 1C), D2 mice ( $n = 5$ ) showed the same pattern of expression for exon 28 A<sup>5</sup>SS ( $p = 0.03$ ), exon 29 (+) ( $p = 0.033$ ), and exon 18 (–) ( $p = 0.046$ ) compared to B6 mice ( $n = 5$ ), but there was no significant strain difference for the 3' UTR ( $p = 0.718$ ) in amygdala. This suggests D2 mice have significantly higher total *Nin* expression compared to B6 mice across most exons, but the decrease in 3'UTR expression in D2 mice predicts an alternative 3'UTR and

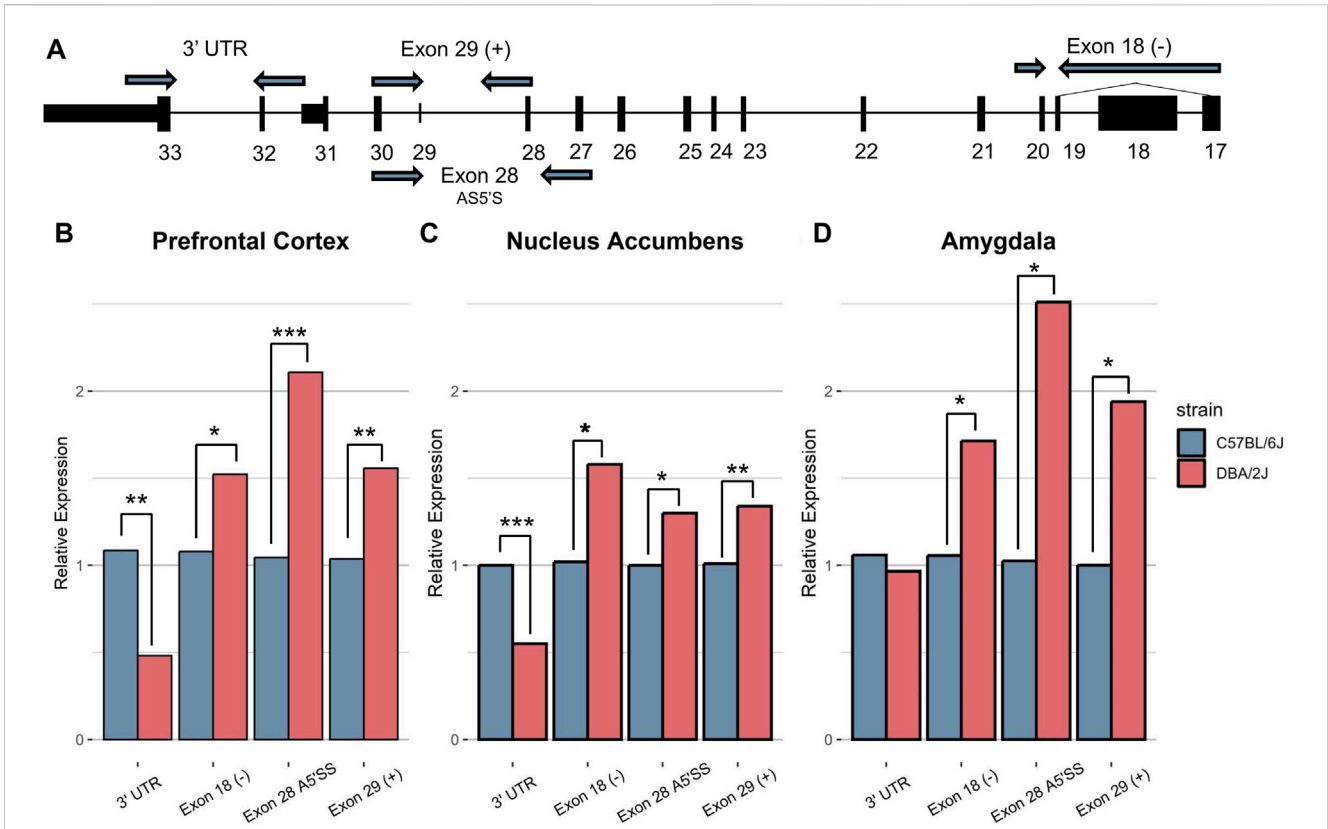


**FIGURE 1** Nin exon-level qRT-PCR. Nin exon-level mRNA expression between B6 and D2 was measured across the (B) prefrontal cortex, (C) nucleus accumbens, and (D) amygdala. (A) Representative image of *Nin* canonical transcript with primer positions. Basal mRNA levels for primers excluding Exon 18, including Exon 29, and using the alternative 5' splice site for Exon 28 were significantly greater in D2 mice than B6 mice across all brain regions (\* $P < 0.01$ , \*\* $P < 0.001$ , \*\*\* $P < 0.0001$ ,  $n = 5-10$  per strain per brain region, Student's  $t$ -test between strains). Primers amplifying the 3' untranslated region (UTR) showed significantly higher expression in B6 mice compared to D2 mice in the PFC and NAc.

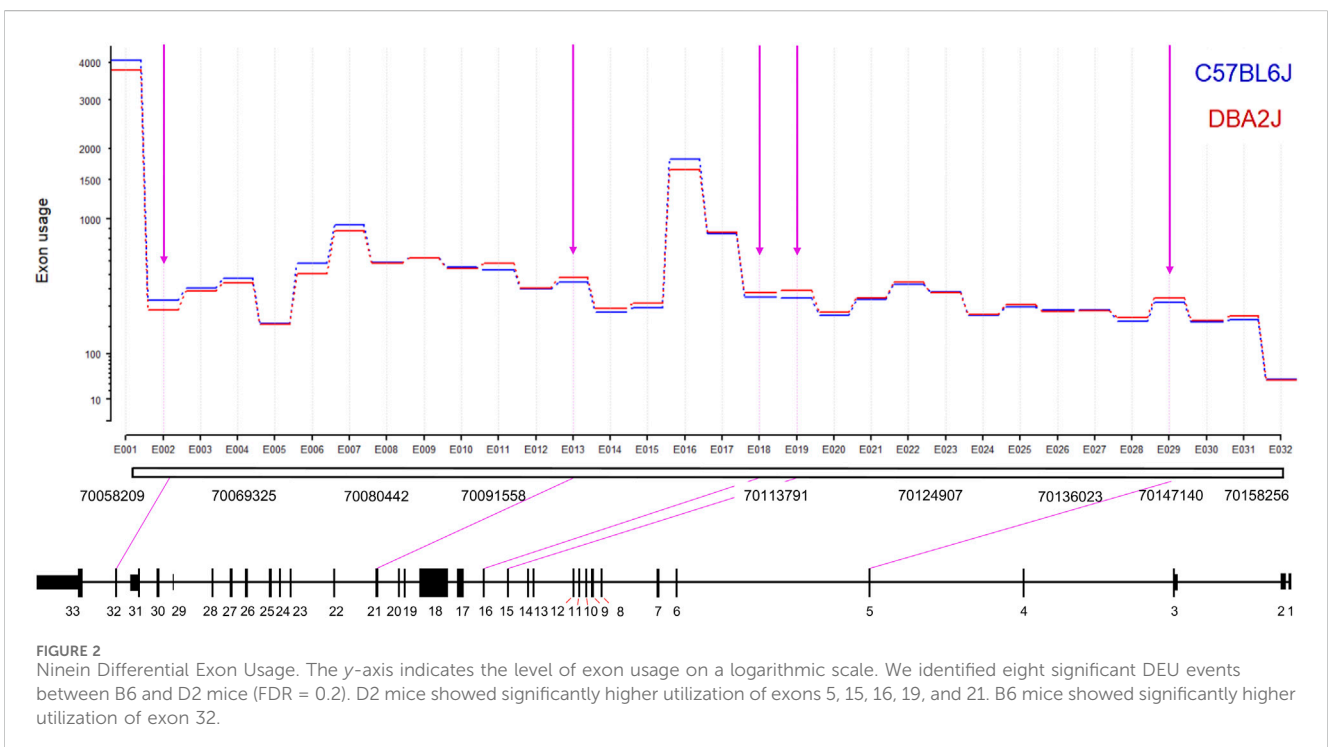


**FIGURE 2** Nin Differential Exon Usage. The y-axis indicates the level of exon usage on a logarithmic scale. We identified eight significant DEU events between B6 and D2 mice (FDR = 0.2). D2 mice showed significantly higher utilization of exons 5, 15, 16, 19, and 21. B6 mice showed significantly higher utilization of exon 32.

**TABLE 1** GeneNetwork *Nin* Exon Phenotype Correlations. *Nin* exon expression was correlated against the top 500 BXD phenotypes from GeneNetwork (Pearson Correlation). Exons showing significant correlation with acute ethanol anxiolysis in the Light Dark Box were identified as exons of interest. Record ID refers to GeneNetwork expression data file number.

Record ID	Exon	Amygdala				Hypothalamus			
		%DTL (EtOH) 5-min		%TIL (EtOH) 5-min		%DTL (EtOH) 5-min		%TIL (EtOH) 5-min	
		Corr.	P-value	Corr.	P-value	Corr.	P-value	Corr.	P-value
10400838	Exon 4	N/A	N/A	-0.601	1.37E-02	-0.695	9.00E-04	-0.7506	3.46E-03
10400837	Exon 5	-0.577	4.96E-03	-0.578	1.91E-02	-0.7367	2.60E-04	-0.7826	1.60E-03
10400836	Exon 6	-0.607	2.72E-03	-0.601	1.39E-02	-0.7453	1.90E-04	-0.8738	5.19E-05
10400835	Exon 7	-0.637	1.44E-03	-0.607	1.26E-02	N/A	N/A	N/A	N/A
10400825	Exon 17	0.623	5.23E-04	0.767	1.96E-03	0.611	5.92E-03	0.672	1.46E-02

greater expression of shortened transcripts in that strain compared to B6 mice.

## Ninein exhibits differential exon usage

To extend the PCR analysis and possibly detect novel transcript variants, we performed deep-read RNA sequencing of the NAc to further evaluate alternative splicing differences between B6 and D2 mice. Differential gene expression analysis with DESeq2 confirmed our *a priori* hypothesis and qRT-PCR data above that D2 mice exhibit significantly higher *Nin* expression compared to B6 ( $\log_2$  fold-change (LFC) = 0.271,  $p_{adj}$  = 5.50685E-07). Full analysis of these D2 v. B6 deep sequencing results will be reported elsewhere (Gnatowski and Miles, in preparation). We then performed an exon-level analysis using DEXSeq to better characterize exon-level expression differences detected by the qRT-PCR (Figure 2; Supplementary Table S3). We used a relaxed statistical threshold ( $FDR \leq 0.2$ ) without LFC filtering to define differential exon usage (DEU) for *Nin*. DEXSeq identified five differentially utilized exons between B6 and D2 mice. Of these five significant DEU events, D2 mice had increased usage of exon 5 ( $p_{adj}$  = 0.175, LFC = 0.11), exon 15 ( $p_{adj}$  = 0.0026, LFC = 0.18), exon 16 ( $p_{adj}$  = 0.153, LFC = 0.105), and exon 21 ( $p_{adj}$  = 0.179, LFC = 0.1), while B6 showed significantly increased usage of exon 32 ( $p_{adj}$  = 0.1104, LFC = -0.245). The increased expression of exon 32 in the B6 mice is consistent with results seen in the qRT-PCR characterization of the transcripts with the full 3' UTR (Figure 1).

## GeneNetwork correlations of Ninein Exons and ethanol-anxiolysis behaviors

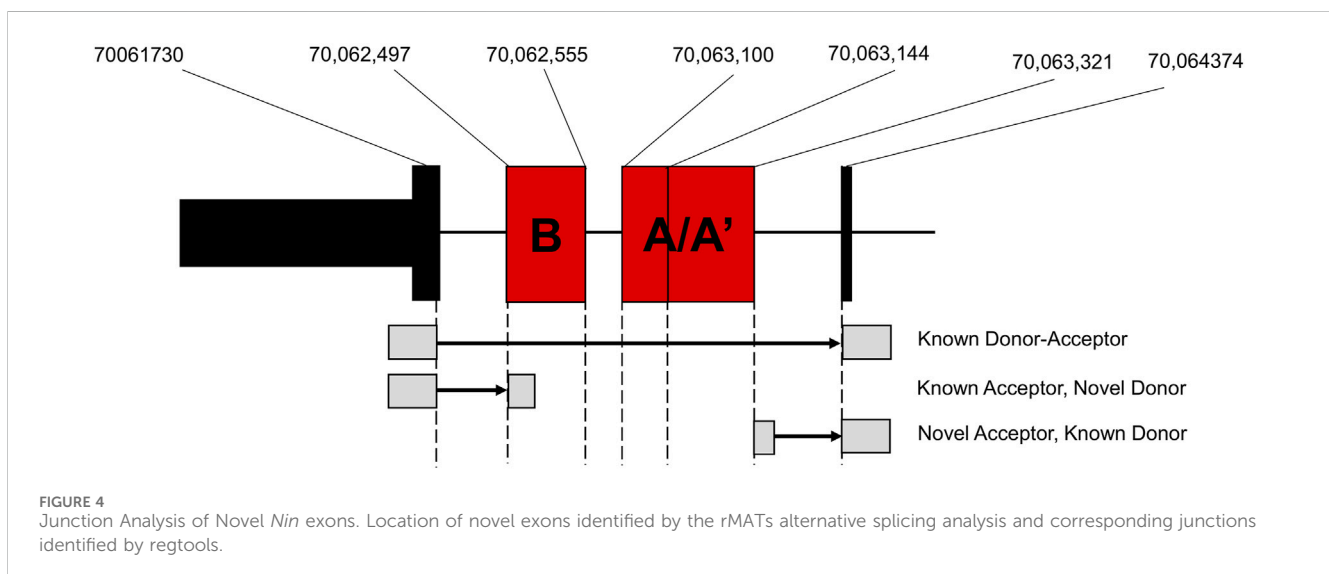
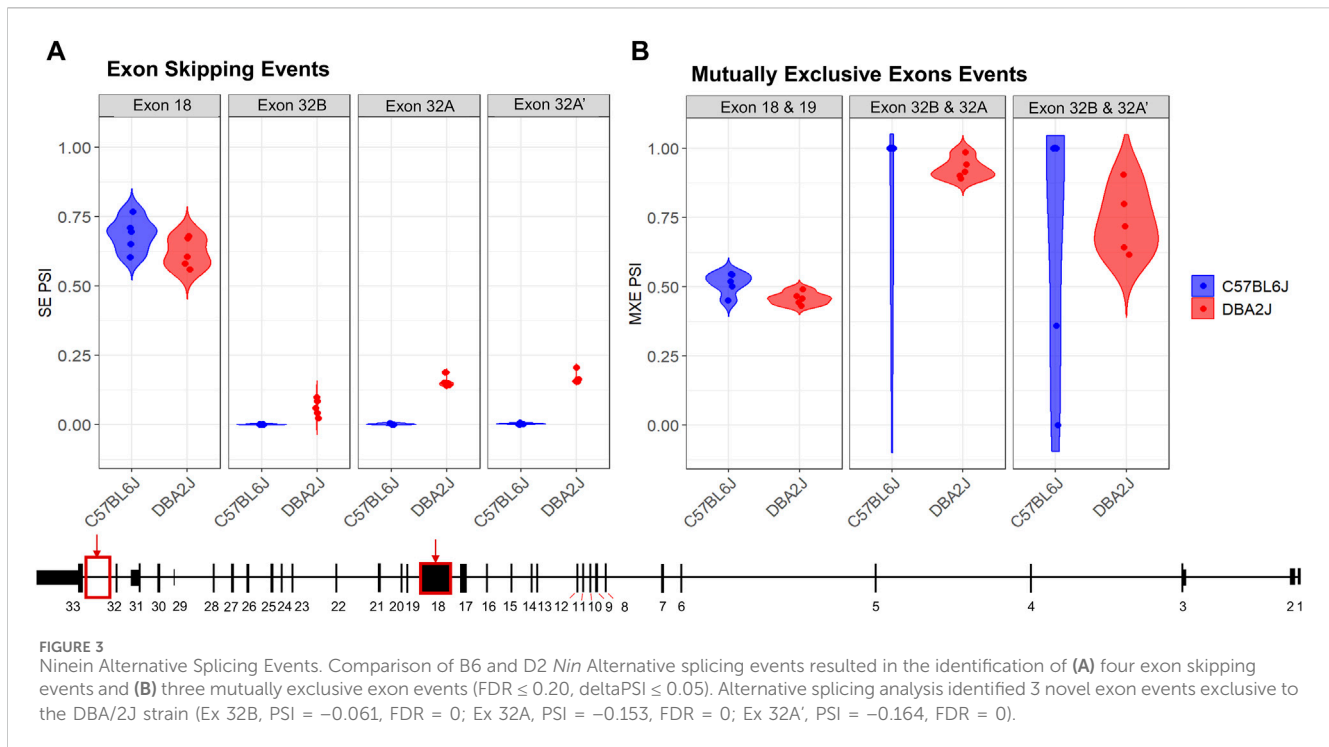
In order to interrogate the relationship between exon-level expression and behavior, we used the GeneNetwork resource to examine correlations in BXD mice between Ninein exon-level expression and our prior acute ethanol anxiolysis behavior (Table 1), given the extensive amount of BXD brain region expression and phenotypic data available at that site. Exon-level expression data for amygdala and hypothalamus, two brain regions known to have roles in stress and anxiety, were available for BXD strains in GeneNetwork and

thus were utilized for this analysis. We identified significant Pearson correlations between the expression of exon four through seven and exon 17 with %TIL in response to acute ethanol in the amygdala (Table 1). %TIL in response to acute ethanol was also significantly correlated with expression of exon four through six and exon 17 in the hypothalamus. We did not see significant correlations between exon seven and %TIL in the hypothalamus after acute ethanol exposure.

We also identified significant Pearson correlations between with exons five through seven and exon 17 in amygdala with %DTL after acute ethanol (Table 1; Supplementary Figure S1). Exon four expression in amygdala was not significantly correlated with %DTL after acute ethanol exposure (Table 1). In the hypothalamus, we identified significant Pearson correlations between %DTL in response to ethanol and expression of exons four through six and exon 17. Hypothalamic exon seven expression showed no significant correlations with %DTL (Table 1). The microarray probe set for Exon eight contained SNPs present in D2 mice that could artificially decrease expression levels in these samples, and thus exon eight data was excluded. These results suggest that the expression of a cluster of *Nin* exons are responsible for the regulation of ethanol anxiolysis in the LDB.

## Ninein exhibits strain-specific alternative splicing

Since Ninein has 18 predicted transcript variants, we used rMATs to analyze strain-specific differences in alternative splicing. An FDR cutoff of  $\leq 0.2$  was employed along with a percent spliced in (PSI,  $\psi$ ) cutoff of  $\psi > 0.05$ . rMATs analysis revealed seven significant alternative splicing events between B6 and D2 mice, including four exon skipping events and three mutually exclusive exons (Figure 3; Supplementary Tables S4, S5). For the exon skipping events, we identified a significant change in  $\psi$  values for the largest exon, exon 18 ( $FDR = 0.177$ ,  $\psi = 0.066$ ), and identified three novel exon skipping events only present in D2 mice occurring between exons 32 and 33 (Figure 3A). These exons will be referred to as 32A ( $FDR < 2.2e-16$ ,  $\Delta\psi = -0.153$ ), 32A' ( $FDR < 2.2e-16$ ,  $\Delta\psi = -0.164$ ), and 32B ( $FDR < 2.2e-16$ ,  $\Delta\psi = -0.061$ ). Exon 32A' represents the alternative 5' splicing of the larger identified exon, exon 32A. These identified exon skipping events overlap with



the identification of transcripts where two exons were deemed mutually exclusive (MXE). Two of these mutually exclusive exon events identified exon 32B to be mutually exclusive from both 32A (FDR = 0.0051) and 32A' (FDR = 0.00092) (Figure 3B). The third alternative splicing exon event showed a significant greater mutually exclusivity between exons 18 and 19 (FDR = 0.0605) in the B6 mice (Figure 3B).

To further investigate these alternative splicing events, we used *regtools* to characterize and quantify reads at novel junctions contributing to novel splicing events. We identified two significant splicing junctions containing either a novel splice acceptor or novel splice donor between exons 32 and 33

(Figure 4; Table 2). The first significant junction identified contains a known splice acceptor on exon 33 (chr12:70,063,321) that spans to the 3' end of identified novel exon 32B (chr12:70,064,347), which contains the novel donor. The second significant junction consists of a novel acceptor site on identified novel exon 32A/A' (chr12:70,061,730) with a known splice donor on Exon 32 (chr12:70,062,498). These findings confirm that the splicing of known coding exons (32 and 33) is occurring at intronic sites specifically in D2 mice.

The identification of these novel splice junctions characterized two independent novel exons, labeled exons 32A and 32B (Figure 5A), with one of these novel exons undergoing

**TABLE 2 Junction Analysis of Novel *Nin* exons.** rMATs was used to quantify reads at known and novel splice junctions. The anchor refers to the type of splice junction identified by rMATs (D = known donor, novel acceptor; A = novel donor, known acceptor; NDA = novel donor, novel acceptor). Student's t-test was ran across all identified novel events and adjusted by Bonferroni correction.

Start	End	Strand	Anchor	Average B6 score	Average D2 score	P-value	Padj.
70063321	70064347	—	D	1.8	77	0.0005	0.003
70061730	70062498	—	A	0.4	22.6	0.003	0.019
70108049	70109463	—	D	2.2	6	0.033	0.196
70109502	70137310	—	NDA	2.2	8	0.134	0.805
70061730	70063101	—	A	0.2	3.4	0.011	0.066

**TABLE 3 *Nin* Exon 18 Ensembl SNPs Between B6 and D2 strains.** SNPs were identified within *Nin* Exon 18 using MGI and Ensembl databases.

SNP ID	Coordinate	Allele summary	B6	D2	Variant type	
rs32227977	70089171	C/T		C	Missense Variant	
rs32227980	70089195	G/T		T	Missense Variant	
rs32227983	70089251	A/G	A	G	Missense Variant	a
rs32228806	70089348	A/G		G	Missense Variant	
rs29183409	70089601	A/G	A	G	Synonymous Variant	
rs32224596	70089643	A/T		T	Synonymous Variant	
rs32224599	70089718	C/T		T	Synonymous Variant	
rs32224602	70089817	C/T		T	Synonymous Variant	
rs32225355	70089904	C/T		C	Synonymous Variant	
rs32225358	70089951	C/T		T	Missense Variant	
rs29202173	70089964	A/G		A	Synonymous Variant	
rs29192398	70090160	C/T	C	T	Missense Variant	a
rs29159683	70090163	G/T	G	T	Missense Variant	
rs32225363	70090252	C/T		T	Synonymous Variant	
rs32226356	70090387	A/G		G	Synonymous Variant	
rs32226359	70090395	C/T		C	Missense Variant	
rs32226362	70090398	C/T		T	Missense Variant	
rs32227145	70090555	C/T		C	Synonymous Variant	
rs29149025	70090689	C/T		C	Missense Variant	
Rs32227150	70090905	A/G		G	Missense Variant	a

<sup>a</sup>predicted deleterious missense variants.

alternative 5' splicing (exon 32A'). We used the Integrative Genome Viewer (IGV) tool to analyze for possible open reading frames of the novel exons identified in the alternative splicing analyses. Figure 5A shows representative B6 and D2 samples to demonstrate the increased sequencing read density between exons 32 and 33 in D2 samples compared to B6 samples. IGV showed an exon present between exons 32 and 33 that aligns with the chromosomal location of the novel exon 32B (chr12:70,062,497–70,062,555) identified by rMATs. This exon contains a short reading frame of five amino acids followed by a termination codon and an alternative 3' UTR (Figure 5B). For exon 32A and its alternative 5' spliced counterpart, exon32A', all theoretical reading frames contained

multiple premature termination codons (Figure 5C). The longest possible reading frame had 46 amino acids prior to a termination codon at chr12:70,063,184. IGV also identified a guanine to adenine (G-A) SNP in the exon 32A region at chr12:70,063,271, however this SNP is a synonymous variant that maintains the status of the potential reading frames.

## PCR validation of novel exons

In order to validate the supporting bioinformatic evidence for the existence of novel exons between exons 32 and 33, we performed





FIGURE 5 Integrative Genome Viewer (IGV) Analysis of Novel Exon Open Reading Frame. (A) Comparison of Read distribution by strain for *Nin* exons 31 through 33. (B) Location of rMATS-identified novel exon 32B (chr12:70,062,497–70,062,555) including amino acid reading frames. (C) Location of rMATS-identified novel exons 32A (chr12:70,063,100–70,063,321) and 32A' (chr12:70,063,144–70,063,321) including amino acid reading frames.

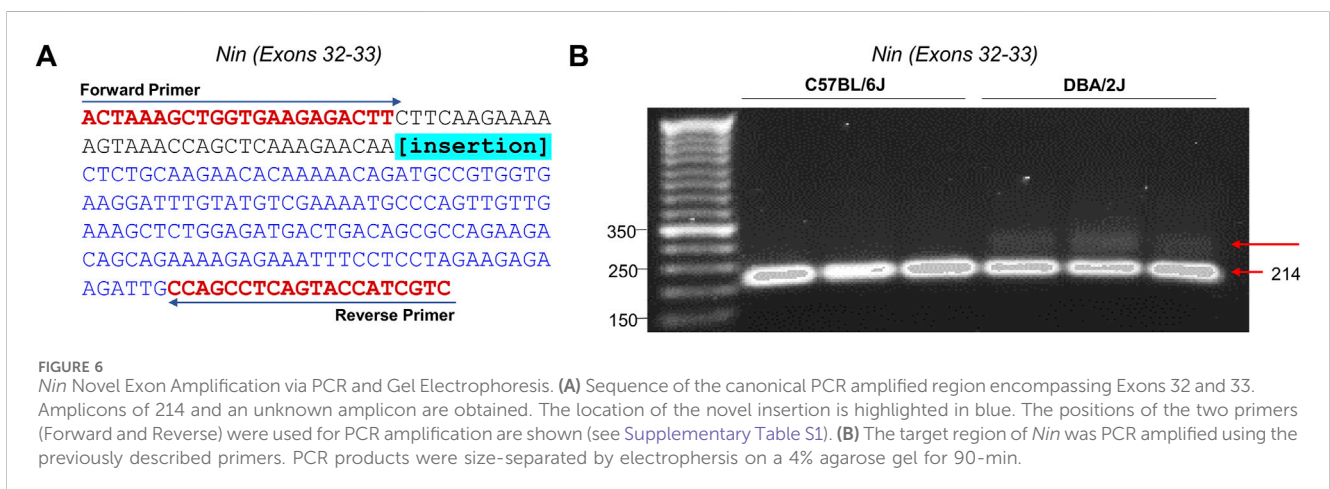


FIGURE 6 *Nin* Novel Exon Amplification via PCR and Gel Electrophoresis. (A) Sequence of the canonical PCR amplified region encompassing Exons 32 and 33. Amplicons of 214 and an unknown amplicon are obtained. The location of the novel insertion is highlighted in blue. The positions of the two primers (Forward and Reverse) were used for PCR amplification are shown (see Supplementary Table S1). (B) The target region of *Nin* was PCR amplified using the previously described primers. PCR products were size-separated by electrophoresis on a 4% agarose gel for 90-min.

RT-PCR targeted at these exons in D2 and B6 nucleus accumbens (Figure 6). PCR primers did not span exon-exon junctions to allow for the amplification between exons 32 and 33 (Figure 6A). cDNA from representative B6 ( $n = 3$ ) and D2 ( $n = 3$ ) were size-separated by electrophoresis on 4% agarose. PCR products from D2 mice yielded two distinct bands: one band served as the representative band for the canonical splicing of exon 32 to exon 33 (214 bp). A second larger band (~250–300 bp) was also identified, consistent with the predicted size of novel exon 32B (Figure 6B). This additional band was not seen in the B6 samples. These results strongly support the existence of an exon exclusive to D2, located in the 3' region of the gene.

## Ninein single nucleotide polymorphisms

We identified 858 SNPs differing between the B6 and D2 strains in the *Nin* gene (chr 12: 70, 058, 297–70,159,961) using the MGI and Ensembl databases (GRCm39) (see Supplementary Table S6). This analysis identified 51 coding region SNPs, with 15 of these identified as missense variants (Table 3). Four of the missense variants were predicted to have “deleterious” effects on the amino acid sequence of the protein based on the SIFT score. Three of these deleterious SNPs occur in exon 18 while the other occurs in exon 27. The other 11 missense SNPs were deemed “tolerated” by the SIFT algorithm, indicating the variant would not greatly impact protein function. Eight of these “tolerated” missense variants also occur within alternatively spliced exon 18. Variants *rs32226359*, *rs32226362*, and *rs29149025* occur in a known enhancer region (ENSMUSR00000789018). We also utilized this database to identify intronic SNPs that correspond to the regions associated with the proposed novel exons in D2 mice. There are 21 intronic SNPs in the region of the proposed novel exons (chr12: 70,061,987–70,063,271) identified in the rMATs alternative splicing analysis. This region corresponds with a known enhancer region (ENSMUSR00000789014) in that area of the gene.

## Discussion

The studies presented here provide the first in-depth analysis of genetic variation in alternative splicing of *Nin*, a candidate gene for ethanol-induced anxiolytic-like behavior. Deep RNA sequencing provided sufficient read depth to characterize strain-differences in exon utilization and alternative splicing events, allowing for the identification of novel strain-specific splicing events. PCR results generally indicated increased total *Nin* expression in D2 mice, but a 50% reduction in *Nin* exon expression in the 3' UTR region of the gene. RNA sequencing both confirmed the increased usage of exon 32 in B6 mice and identified novel splicing events between exons 32 and 33. The novel splicing events shown here pose the possibility of the use of alternative 3' untranslated regions by the D2 mice which would result in truncated NIN protein isoforms. Our findings also showed increased exon skipping of the largest exon, exon 18, in D2 mice, which may occur as a consequence of the D2 strain containing three deleterious SNPs in this coding exon. The alternative splicing events characterized here may provide a genetic mechanism for strain specific regulation of *Nin*

transcription that contributes to behavioral differences in the anxiolytic response to an acute dose of ethanol between B6 and D2 mice. These results also provide further support for *Nin* being a candidate gene underlying the *Etanq1* QTL previously identified by our laboratory associated with ethanol anxiolytic-like activity in BXD mice (Putman et al., 2016).

## Exon-level expression and behavioral correlations

Alternative splicing is a crucial step of post-transcriptional gene expression that substantially increases transcriptome diversity and is critical for diverse cellular processes, including cell differentiation, development, cellular localization, and tissue remodeling (Mulligan et al., 2017; Shen et al., 2014). Differential exon usage comes as a result of increased exon skipping, the most prevalent form of alternative splicing, leading to the selective inclusion or exclusion of coding regions during the formation of mRNA (Ule and Blencowe, 2019). It has been proposed that RNA alternative splicing, specifically exon skipping, plays a causal role in Alcohol Use Disorder (AUD) susceptibility (Yeo et al., 2004). Our DEXSeq analysis identified five differential exon usage events where one of these events overlapped with exon 5, which showed significant correlations with phenotypes from the anxiolytic response to ethanol previously identified in Putman et al. (Putman et al., 2016). Exon five showed significant negative correlations with % TIL and %DTL in the light dark box in both the amygdala and hypothalamus, indicating that higher *Nin* exon five expression would result in a decreased anxiolytic response to ethanol. This correlation appears to pool in a strain-dependent manner where BXD strains with the B6 allele have decreased *Nin* expression (see Supplementary Figure S1). This is consistent with DEU results showing B6 mice have lower exon five usage compared to D2 mice. This highlights exons 5 as an exon-specific target underlying an ethanol-responsive candidate gene.

## Exon 18 skipping

Ninein (*Nin*) is an exceptionally large gene containing 33 protein coding exons, generating protein products that can vary in an isoform-dependent manner. Previous work from Zhang and colleagues elucidated the role of alternative splicing of the *Nin* gene in the differentiation of neural progenitor cells (NPCs) into mature neurons (Zhang et al., 2016). They pinpointed two exons that play pivotal roles in this process. The first, a 61-nucleotide exon (exon 29), is specifically expressed in neurons but excluded in NPCs. The inclusion of this exon triggered the dissociation of *Nin* from the centrosomal protein CEP250, leading to *Nin* diffusion into the cytoplasm. Conversely, those investigators found that the exclusion of a larger exon (exon 18, >2,000 nucleotides) in mature neurons, that is not present in NPCs, resulted in the dissociation of another centrosomal protein, CEP170, from NIN (Zhang et al., 2016). Zhang and colleagues argued that these alternative splicing events appeared sufficient to differentiate NPCs into neurons. Our initial characterization of *Nin* alternative splicing using qRT-PCR showed that compared to B6,

D2 mice have increased expression of transcripts containing exon 29 and transcripts excluding exon 18. This suggests that D2 mice have higher expression of non-centrosomal *Nin* splice variants. This initial result was corroborated by the alternative splicing analysis that indicated exon 18 exhibited significantly greater exon skipping in D2 mice. The decreased utilization of exon 18 in D2 mice may ultimately contribute to decreased localization of CEP170 to the centrosome and increased NPC differentiation into mature neurons.

The underlying mechanism for D2 mice having a lower rate of exon 18 utilization is unknown. However, SNP analysis identified 11 missense variant SNPs in exon 18 alone of D2 mice, three of which were predicted “deleterious” SNPs that would result in a change in the protein structure leading to loss of function or harmful gain of function (Yue and Moul, 2006). This could drive increased splicing out of exon 18 in D2 mice. However, even for *Nin* splice variants containing exon 18 in D2 mice, those proteins might not be fully functional in terms of centrosomal localization. The net result of decreased exon 18 utilization and probable decreased exon 18 function in D2 mice seems likely to impair *Nin* centrosome localization or function in non-neuronal cells and might lead to developmental alterations in the relative abundance of neurons in D2 mice given the role of *Nin* in neuronal differentiation. However, further confirmation of such differences between B6 and D2 mice at a cellular level is needed.

## Identification of novel exons and alternative 3' UTRs

Another major finding from these studies is the identification of novel exons between exons 32 and 33 specifically expressed only in D2 mice. Our original findings from the qRT-PCR results looking at *Nin* exon expression highlighted a 50% reduction in the expression of the exon 32 to the 3' UTR in D2 mice compared to B6 mice. This result was corroborated by the DEU results indicating that exon 32 has higher exon usage in B6 mice. Confirmation of the presence of these novel exons by PCR gel electrophoresis identified a second band exclusive to D2 mice consistent in size with inclusion of novel exon 32B, which contains an alternative stop codon and 3' UTR. Together, these results indicate that D2 mice uniquely produce shortened *Nin* mRNA transcripts with alternate 3' UTRs and an altered carboxy terminus of the protein coding region. It remains unclear whether or not the identification of novel exons 32A and 32A' result in the inclusion of an additional 3' UTR, or whether or not the inclusion of these exons leads to the increased utilization of a 3'UTR region following exon 31 shown in Figure 5A. This would be consistent with the lack of an additional band in the gel electrophoresis 177–221 bp higher than the known band.

## 3' UTR- localization

The 3' untranslated region (3' UTR) plays a pivotal role in post-transcriptional modulation of gene expression. The 3' UTR often contains regulatory regions that influence gene expression by

regulating processes such as polyadenylation, translation efficiency, localization, and stability of the mRNA (Mayya and Duchaine, 2019; Mitschka and Mayr, 2022). Given the *Nin* alternative exon usage in D2 mice noted above, it is possible that the alternative 3' UTRs could change *Nin* mRNA localization or function. Transcripts containing multiple 3' UTRs encoding the same protein have been repeatedly reported. For example, mRNAs for *BDNF* containing the same coding sequence with different 3' UTRs resulted in distinct differences in localization where the long 3' UTR localized BDNF to distal dendrites and shorter 3' UTR *BDNF* transcripts remained in the soma (Anders et al., 2012). Similar examples have been reported for *CamK2a* (Rook et al., 2000). Of note, our prior studies on mRNA localization to synaptoneuroosomes indicated increased *Nin* mRNA abundance in the cellular fraction containing pre- or post-synaptic contents in D2 mice (O'Brien et al., 2018). In the case of *Nin*, the usage of alternative 3' UTRs may provide a genetic mechanism for the regulation of *Nin* trafficking and function in dendritic microtubule polarity, however the exact transcript altering this localization is unclear (Mitschka and Mayr, 2022). The localization of microtubules in dendrites may also contribute to changes in the trafficking of GABA and glycine receptors to the postsynaptic site (Anders et al., 2012; Parato and Bartolini, 2021). This highlights a specific cellular signaling mechanism by which *Nin* expression and splicing could modulate ethanol's anxiolytic properties.

## Conclusion

This study is the first to provide an in-depth genomic and bioinformatic analysis of a QTL-identified candidate gene for ethanol anxiolytic activity. We observed strain-specific differences in exon regulation across different analysis parameters that we hypothesize played a critical role in regulating ethanol anxiolysis that lead to the identification of *Nin* as a candidate gene. The alternative splicing events that we identified could alter localization and expression of the NIN protein. *In vivo* confirmatory studies examining deletion or modification of specific *Nin* exons are needed to further validate the contribution of specific exons in regulating *Nin* localization and expression and, ultimately, in confirming the function of different *Nin* transcripts in modulating strain-specific ethanol behavioral differences.

## Data availability statement

The original contributions presented in the study are publicly available. This data can be found here: <https://www.ncbi.nlm.nih.gov/geo/query/acc.cgi?acc=GSE274854>.

## Ethics statement

The animal study was approved by Institutional Animal Care and Use Committee of Virginia Commonwealth University. The study was conducted in accordance with the local legislation and institutional requirements.

## Author contributions

EG: Conceptualization, Formal Analysis, Writing–review and editing, Data curation, Investigation, Methodology, Visualization, Writing–original draft. JJ: Writing–review and editing, Investigation, Methodology. MD: Methodology, Writing–review and editing. JW: Methodology, Writing–review and editing. MM: Conceptualization, Formal Analysis, Funding acquisition, Methodology, Project administration, Resources, Supervision, Writing–review and editing.

## Funding

The author(s) declare that financial support was received for the research, authorship, and/or publication of this article. This work was supported by grants F31AA030727 (ERG), P50AA022537 (MFM), and R01AA027581 (MFM) from the National Institute on Alcohol Abuse and Alcoholism.

## Acknowledgments

The data included in this study was generated at the Genomics Core facility at Virginia Commonwealth University. We would like to thank Kalyan Mallempati for cDNA library preparation and running the RNA-sequencing, and members of the MM

## References

- Anders, S., Reyes, A., and Huber, W. (2012). Detecting differential usage of exons from RNA-seq data. *Genome Res.* 22, 2008–2017. doi:10.1101/gr.133744.111
- Baird, D. H., Myers, K. A., Mogensen, M., Moss, D., and Baas, P. W. (2004). Distribution of the microtubule-related protein ninein in developing neurons. *Neuropharmacology* 47, 677–683. doi:10.1016/j.neuropharm.2004.07.016
- Baldarelli, R. M., Smith, C. M., Finger, J. H., Hayamizu, T. F., McCright, I. J., Xu, J., et al. (2021). The mouse gene expression database (GXD): 2021 update. *Nucleic Acids Res.* 49, D924–D931. doi:10.1093/nar/gkaa914
- Becker, H. C. (2017). Influence of stress associated with chronic alcohol exposure on drinking. *Neuropharmacology* 122, 115–126. doi:10.1016/j.neuropharm.2017.04.028
- Belknap, J. K., Crabbe, J. C., and Young, E. R. (1993). Voluntary consumption of ethanol in 15 inbred mouse strains. *Psychopharmacology* 112, 503–510. doi:10.1007/BF02244901
- Bigdeli, T. B., Fanous, A. H., Li, Y., Rajeevan, N., Sayward, F., Genovese, G., et al. (2021). Genome-wide association studies of schizophrenia and bipolar disorder in a diverse cohort of US veterans. *Schizophr. Bull.* 47, 517–529. doi:10.1093/schbul/sbaa133
- Blake, J. A., Baldarelli, R., Kadin, J. A., Richardson, J. E., Smith, L., Cynthia, Bult, C. J., et al. (2021). Mouse Genome Database (MGD): knowledgebase for mouse–human comparative biology. *Nucleic Acids Res.* 49, D981–D987. doi:10.1093/nar/gkaa1083
- Chen, S., Zhou, Y., Chen, Y., and Gu, J. (2018). fastp: an ultra-fast all-in-one FASTQ preprocessor. *Bioinformatics* 34, i884–i890. doi:10.1093/bioinformatics/bty560
- Cotto, K. C., Feng, Y. Y., Ramu, A., Richters, M., Freshour, S. L., Skidmore, Z. L., et al. (2023). Integrated analysis of genomic and transcriptomic data for the discovery of splice-associated variants in cancer. *Nat. Commun.* 14, 1589. doi:10.1038/s41467-023-37266-6
- Dobin, A., and Gingeras, T. R. (2016). Optimizing RNA-seq mapping with STAR. *Methods Mol. Biol.* 1415, 245–262. doi:10.1007/978-1-4939-3572-7\_13
- Farris, S. P., Harris, R. A., and Ponomarev, I. (2015). Epigenetic modulation of brain gene networks for cocaine and alcohol abuse. *Front. Neurosci.* 9, 176. doi:10.3389/fnins.2015.00176
- Goldspink, D. A., Rookyard, C., Tyrrell, B. J., Gadsby, J., Perkins, J., Lund, E. K., et al. (2017). Ninein is essential for apico-basal microtubule formation and CLIP-170 facilitates its redeployment to non-centrosomal microtubule organizing centres. *Open Biol.* 7, 160274. doi:10.1098/rsob.160274
- Heilig, M., Egli, M., Crabbe, J. C., and Becker, H. C. (2010). Acute withdrawal, protracted abstinence and negative affect in alcoholism: are they linked? *Addict. Biol.* 15, 169–184. doi:10.1111/j.1369-1600.2009.00194.x
- Kerns, R. T., Ravindranathan, A., Hassan, S., Cage, M. P., York, T., Sikela, J. M., et al. (2005). Ethanol-responsive brain region expression networks: implications for behavioral responses to acute ethanol in DBA/2J versus C57Bl/6J mice. *J. Neurosci.* 25, 2255–2266. doi:10.1523/JNEUROSCI.4372-04.2005
- Kinjo, S., Monma, N., Misu, S., Kitamura, N., Imoto, J., Yoshitake, K., et al. (2018). Maser: one-stop platform for NGS big data from analysis to visualization. *Database (Oxford)* 2018, bay027. doi:10.1093/database/bay027
- Lee, Y., and Rio, D. C. (2015). Mechanisms and regulation of alternative pre-mRNA splicing. *Annu. Rev. Biochem.* 84, 291–323. doi:10.1146/annurev-biochem-060614-034316
- Liao, Y., Smyth, G. K., and Shi, W. (2014). featureCounts: an efficient general purpose program for assigning sequence reads to genomic features. *Bioinformatics* 30, 923–930. doi:10.1093/bioinformatics/btt656
- Li, H., Handsaker, B., Wysoker, A., Fennell, T., Ruan, J., Homer, N., et al. (2009). The sequence alignment/map format and SAMtools. *Bioinformatics* 25, 2078–2079. doi:10.1093/bioinformatics/btp352
- Love, M. I., Huber, W., and Anders, S. (2014). Moderated estimation of fold change and dispersion for RNA-seq data with DESeq2. *Genome Biol.* 15, 550. doi:10.1186/s13059-014-0550-8
- Martin, F. J., Amode, M. R., Aneja, A., Austine-Orimoloye, O., Azov, G., Barnes, I., et al. (2023). Ensembl 2023. *Nucleic Acids Res.* 51, D933–D941. doi:10.1093/nar/gkac958
- Mayya, V. K., and Duchaine, T. F. (2019). Ciphers and executioners: how 3′-untranslated regions determine the fate of messenger RNAs. *Front. Genet.* 10, 6. doi:10.3389/fgene.2019.00006
- Mitschka, S., and Mayr, C. (2022). Context-specific regulation and function of mRNA alternative polyadenylation. *Nat. Rev. Mol. Cell Biol.* 23, 779–796. doi:10.1038/s41580-022-00507-5
- Mogensen, M. M., Malik, A., Piel, M., Bouckson-Castaing, V., and Bornens, M. (2000). Microtubule minus-end anchorage at centrosomal and non-centrosomal sites: the role of ninein. *J. Cell Sci.* 113, 3013–3023. doi:10.1242/jcs.113.17.3013

laboratory for helpful discussions in the preparation of this manuscript.

## Conflict of interest

The authors declare that the research was conducted in the absence of any commercial or financial relationships that could be construed as a potential conflict of interest.

## Publisher's note

All claims expressed in this article are solely those of the authors and do not necessarily represent those of their affiliated organizations, or those of the publisher, the editors and the reviewers. Any product that may be evaluated in this article, or claim that may be made by its manufacturer, is not guaranteed or endorsed by the publisher.

## Supplementary material

The Supplementary Material for this article can be found online at: <https://www.frontiersin.org/articles/10.3389/fgene.2024.1455616/full#supplementary-material>

- Mulligan, M. K., Mozhui, K., Prins, P., and Williams, R. W. (2017). GeneNetwork: a toolbox for systems genetics. *Methods Mol. Biol.* 1488, 75–120. doi:10.1007/978-1-4939-6427-7\_4
- Nikom, D., and Zheng, S. (2023). Alternative splicing in neurodegenerative disease and the promise of RNA therapies. *Nat. Rev. Neurosci.* 24, 457–473. doi:10.1038/s41583-023-00717-6
- O'Brien, M. A., Weston, R. M., Sheth, N. U., Bradley, S., Bigbee, J., Pandey, A., et al. (2018). Ethanol-induced behavioral sensitization alters the synaptic transcriptome and exon utilization in DBA/2J mice. *Front. Genet.* 9, 402. doi:10.3389/fgene.2018.00402
- Parato, J., and Bartolini, F. (2021). The microtubule cytoskeleton at the synapse. *Neurosci. Lett.* 753, 135850. doi:10.1016/j.neulet.2021.135850
- Putman, A. H., Wolen, A. R., Harenza, J. L., Yordanova, R. K., Webb, B. T., Chesler, E. J., et al. (2016). Identification of quantitative trait loci and candidate genes for an anxiolytic-like response to ethanol in BXD recombinant inbred strains. *Genes Brain Behav.* 15, 367–381. doi:10.1111/gbb.12289
- Ribeiro, E. A., Scarpa, J. R., Garamszegi, S. P., Kasarskis, A., Mash, D. C., and Nestler, E. J. (2017). Gene network dysregulation in dorsolateral prefrontal cortex neurons of humans with cocaine use disorder. *Sci. Rep.* 7, 5412. doi:10.1038/s41598-017-05720-3
- Rook, M. S., Lu, M., and Kosik, K. S. (2000). CaMKIIalpha 3' untranslated region-directed mRNA translocation in living neurons: visualization by GFP linkage. *J. Neurosci.* 20, 6385–6393. doi:10.1523/JNEUROSCI.20-17-06385.2000
- Schuckit, M. A., and Hesselbrock, V. (1994). Alcohol dependence and anxiety disorders: what is the relationship? *Am. J. Psychiatry* 151, 1723–1734. doi:10.1176/ajp.151.12.1723
- Schuckit, M. A., and Smith, T. L. (1997). Assessing the risk for alcoholism among sons of alcoholics. *J. Stud. Alcohol* 58, 141–145. doi:10.15288/jsa.1997.58.141
- SHEN, S., PARK, J. W., LIN, L., HENRY, M. D., WU, Y. N., ZHOU, Q., et al. (2014). rMATS: Robust and flexible detection of differential alternative splicing from replicate RNA-Seq data. *Biological Sciences*. 111, E5593–E5601.
- Ule, J., and Blencowe, B. J. (2019). Alternative splicing regulatory networks: functions, mechanisms, and evolution. *Mol. Cell* 76, 329–345. doi:10.1016/j.molcel.2019.09.017
- Wang, Y., Liu, J., Huang, B., Xu, Y.-M., Li, J., Huang, L.-F., et al. (2015). Mechanism of alternative splicing and its regulation. *Biomed. Rep.* 3, 152–158. doi:10.3892/br.2014.407
- Yeo, G., Holste, D., Kreiman, G., and Burge, C. B. (2004). Variation in alternative splicing across human tissues. *Genome Biol.* 5, R74. doi:10.1186/gb-2004-5-10-r74
- Yue, P., and Moul, J. (2006). Identification and analysis of deleterious human SNPs. *J. Mol. Biol.* 356, 1263–1274. doi:10.1016/j.jmb.2005.12.025
- Zhang, X., Chen, M. H., Wu, X., Kodani, A., Fan, J., Doan, R., et al. (2016). Cell-type-specific alternative splicing governs cell fate in the developing cerebral cortex. *Cell* 166, 1147–1162. doi:10.1016/j.cell.2016.07.025